EXPLORING THE LIMITS OF MULTI-ANTENNA SIGNAL-REJECTION FOR GNSS RECEIVERS

James T. Curran, Michele Bavaro, Joaquim Fortuny

European Commission, Joint Research Centre (JRC),
Institute for the Protection and Security of the Citizen (IPSC), Italy.
james.curran@, michele.bavaro @, joaquim.fortuny@jrc.ec.europa.eu

ABSTRACT

This paper presents experimental results exploring the performance of GNSS receivers equipped with controlled radiation pattern antennas. Experiments focus on identifying those features and characteristics of their implementation that may limit the achievable performance of signal-rejection techniques. The study describes both conductive and broadcast experiments conducted in a large anechoic chamber and computer-based Monte-Carlo simulations. Results include a precise gain pattern measurement of a typical antenna array, an investigation and comparison of both analogue RF and digital IF null steering along with some novel theoretical results.

INTRODUCTION

Directional antennas offer a powerful means of achieving signal selectivity when various signal sources observed by a receiver are separated spatially. In the context of GNSS, which must accommodate a mobile receiver, observing many moving transmitters, controlled radiation pattern antennas are an attractive option. Indeed, antenna arrays have been exploited extensively in GNSS receivers both for signal rejection, such as interference and multi-path mitigation or anti-spoofing; and for the purposes of gain enhancement, angle-of-arrival, or attitude estimation.

A number of different factors can influence the achievable levels of signal rejection using antenna arrays. These factors include: the gain and phase stability of the analogue RF and IF stages; the linearity of the analogue stages; and fidelity of the digital stages. Seeking to identify the bound imposed by each of these limiting factors, this paper explores the limits of signal rejection using antenna arrays. The study considers a circular antenna array, consisting of seven passive dual-polarized (RHCL/LHCP) L1-L2 elements. Two types of element combining techniques are examined: one being the analogue combination of signals at RF via a bank of controllable phase shifters and attenuators; the other being the digital combining of IF signals immediately after digitization. Broadcast experiments are conducted in large diameter anechoic chamber, housing a rotatable central pillar, upon which the array is mounted, and two broadcast antennas mounted on movable sleds.

The results presented here include the a precise three dimensional phase and gain calibration of the antenna array using an Agilent network analyser, to explore the properties of antenna elements when placed in close proximity on a common ground plane. Further results include an investigation of the nulling depth achievable by the array via the synchronous broadcast of two GNSS-like CDMA signals, from different broadcast antenna. These results are then extrapolated to infer the relative degradation in nulling capability when the receivers estimate of the amplitude and phase of the signal to be rejected is poor. Thirdly, a comparison of analogue and digital element combining is explored, with emphasis on the rejection of strong jamming signals. This experiment seeks to illustrate and quantify the unique benefits and limitations of each technique. In particular noting that analogue combining enjoys high linearity and can accommodate high interference power, but is typically restricted to the use coarse phase and gain coefficients when combining elements. In contrast, digital combining can offer notably higher gain and phase resolution, but is limited by the dynamic range of the digitizer.

ANTENNA CHARACHTERISTICS

This work has focused on the use of a seven-element circular antenna array, consisting of Antcom dual-polarized, RHCP and LHCP, dual frequency, L1 and L2 elements [1]. The antenna elements are mounted on a single circular aluminum ground plane 2 mm in thickness and 50 cm in diameter, and placed in a hexagonal arrangement at a spacing of 12.5 cm, as depicted in Figure 2. Because the antennas are passive, and can be used both for transmission and for reception, characterization tests were be performed in broadcast mode while the typical receive-mode operation of the array is performed using an in-line Tallysman LNA after the antenna [2].

Experiments described here were conducted in an anechoic chamber, hemispherical in shape with a diameter of 20 m, as depicted in Figure 2. The array was mounted on a surveyors tripod, as shown in Figure 1, and placed at a known

position on a rotatable pillar at the center of the chamber. The chamber contains two sleds, Sled-A and B, that that can be precisely positioned along an arc through the zenith at positions between ±115° either size of the vertical. These antennas include 1.0 to 6.0 GHz vertical and horizontally polarized standard-gain horn antennas.

As the characteristics of antenna array itself is central to the ultimate performance of beamforming or null-steering techniques, a thorough characterization of the gain and phase properties of each of the seven antenna elements was conducted. To do so, an Agilent network analyzer was used to observe the gain and phase response of the antenna under test from a range of observation angles [3]. The array was operated in transmit mode a signal sourced from Port-A of the network analyzer, which was received by an antenna mounted on one of the movable sleds, and fed to Port-B of the network analyzer. The network analyzer was configured to broadcast a series of 201 equally spaced tones spanning 20 MHz centered at 1575.42 MHz at a power of -7 dBm from the antenna array. A mechanical RF multiplexer was used to implement a time-division multiplexing of this broadcast measurement signal across each of the seven elements, such that the series of tones were transmitted once per antenna element. By performing the scan for each antenna element, for a range of positions of Sled-A, and repeating this for different rotations of the central pillar, a precise frequency response could be calculated for a large set of points across the entire upper hemisphere of the antenna. The scan was computed on signals received by both the horizontal and vertical elements on Sled-A, such that both the RHCP and LHCP response are computed. The vertical cuts of this gain pattern were measured with resolution of 2°, while the horizontal cuts were measured with a resolution of 5°. By combining the measured response at both the vertical and horizontal elements on Sled-A.

The average gain response, calculated across the 20 MHz band, for each of the seven elements is depicted in Figure 1. It is interesting to note that the gain pattern exhibited by each element is sensitive to its position on the ground plane, and its position relative to other elements. Two distinct patterns are present, that of the central element (element 1) and that of the peripheral elements (elements 2-7). The central element is circularly symmetric with a single lobe in the direction of the zenith, while gain of the peripheral elements is deflected outwards, having lower gain across the center of the array, and an increased gain for high elevations away from the center of the array. The difference in gain pattern across elements is stark and should, perhaps, influence the choice of elements to be used when forming a beam or null in a given direction, one or other of the signals should be scaled to compensate for this gain difference.

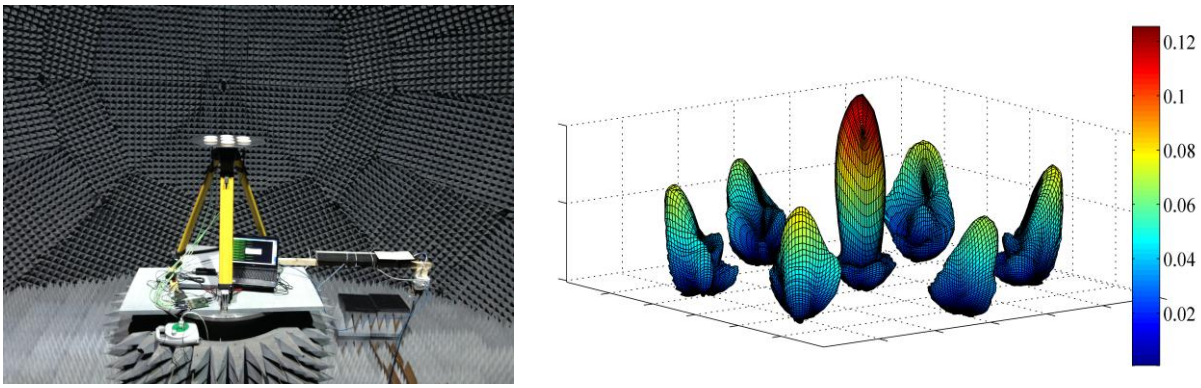

Figure 1: Antenna array and digitizing front-end in the anechoic chamber during broadcast testing (left), and the measured gain pattern of each of the seven elements in the antenna array (right).

PRECISE MEASUREMENT OF SIGNAL REJECTION

Two methods of controlling the antenna radiation pattern are examined here: that of analogue combining of RF signals via a bank of controllable attenuators and phase-shifters; and that of the combining of IF signals after the down conversion and digitization stages. Before exploring the unique benefits and drawbacks of each approach, an analysis of the achievable performance of the array was conducted, in order to identify if there is any underlying limitation to the capability of the array, and to investigate the achievable performance as a function of signal parameter estimation. The nulling performance of the system was examined in terms of its and the rejection capability: assessed of the relative received power of signal of interest, *b(t)*, that is to be preserved, and an unwanted signal, *a(t)*, which is to be rejected, before and after the nulling combination. If $s_i(t)$ denotes some signal as received at antenna *i*, then combination of the signals received at antennas *i* and *j* can be denoted by:

$$C_{i,j}(s,\kappa,\phi) = s_i(t) + \kappa e^{j\phi} s_j(t)\,, \tag{1}$$

where κ and ϕ respectively represent a scaling gain and a phase rotation to be applied. When intending to form a beam in the direction of the source of *s(t)*, then this phase might be chosen to bring $s_j(t)$ into alignment with $s_i(t)$ and the gain may be determined as a function of the signal-to-noise ratio at each antenna, or simply set to unity. In contrast, when it is intended to reject *s(t)* then ϕ must be chosen to place $s_j(t)$ in antiphase with $s_i(t)$ and κ must be chosen to scale the amplitude of $s_j(t)$ to be exactly equal to that of $s_i(t)$.

In this case we consider the problem of placing a null in the direction of signal *a(t)* while preserving signal *b(t)*. If the relative received power of *a(t)* and *b(t)* at antenna *i* is taken as a reference, then the rejection of *a(t)* with respect to *b(t)*, denoted $R_{a,b}$, can be assessed by examining the change in relative power after the null has been placed:

$$R_{a,b} = \frac{\left\langle |a|^2(t) \right\rangle}{\left\langle |b|^2(t) \right\rangle} \frac{\left\langle \left| C_{i,j}(b, \kappa, \pi + \phi) \right|^2(t) \right\rangle}{\left\langle \left| C_{i,j}(a, \kappa, \pi + \phi) \right|^2(t) \right\rangle}, \tag{2}$$

where $\langle x \rangle$ denotes the expected value of *x*. Note also that this convention implies that a value of $R_{a,b}$ greater than unity corresponds to signal rejection.

In practice, multiple signals are received at the same antenna and, so, extracting a measurement of the power of an individual signal, *s(t)*, is not always possible unless some means of isolating one signal amongst the ensemble is available. To facilitate such measurement, this experiment has chosen *a(t)* and *b(t)* to be CDMA signals, modulated by very long direct-sequence orthogonal codes. Specifically, each signal have been modulated by a primary, secondary and tertiary code, each of which has a length of 1023 chips. The primary code has a rate of 1.023 Mcps; the secondary code produces one chip per period of the primary code and, therefore has a rate of 1.0 kcps; while the tertiary code produces one chip per period of the secondary code, and therefore has a rate of approximately 977.5 mcps. The standard GPS L1 C/A PRN sequences have been chosen for the codes, with signal *a(t)* respectively using PRN 1, 2 and 3, for the primary, secondary and tertiary codes, and signal *b(t)* using PRN 4, 5 and 6.

The benefit of this experimental setup is that *a(t)* and *b(t)* can be respectively broadcast from Sleds A and B, at same power, and that the correlation gain and cross-correlation protection can be exploited to independently observe the received signal strength of each signal, at each antenna. Note the importance that this this can be done without driving the analogue or digital receiver elements out of their linear range of operation. Furthermore, as the composite cross-correlation protection of the three codes is very large, the residual strength of the nulled signal can also be observed even for very deep nulling. The exact cross correlation protection depends on the specific codes, their alignment and the observation period, however a conservative estimate suggests that over an observation period of one second, covering the primary and secondary codes, a protection in excess of 48 dB should be achieved; with this extending to 72 dB with the inclusion of the entire tertiary code. This implies that if having placed a null to reject *a(t)*, then its residual power after nulling can be isolated from that of *b(t)*, and reliably measured, for rejection levels up to approximately 72 dB. Beyond this point it is likely that the residual power of signal *a(t)* is indistinguishable from that of the cross-correlation power with *b(t)*. In practice, however, it is likely that the true cross-correlation protection is higher than this limit [4].

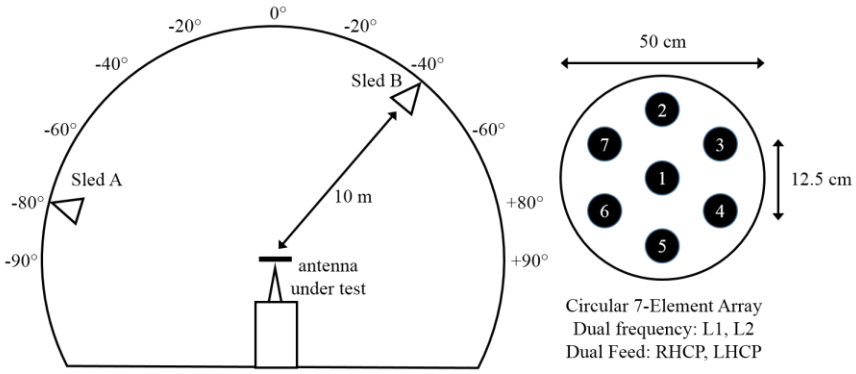

Figure 2: Layout of the antenna under test, and the two movable transmit antennas, respectively denoted *Sled A* and *Sled B* (left), and the layout of the seven element circular array, indicating hexagon dimension and element placement (right).

The tests signals, *a(t)* and *b(t)*, were synthesized in software to produce two sets of complex baseband samples, of 14-bit resolution at a rate of 5.0 MHz. These were then broadcast from a national instruments PXI chassis hosting two RFSG vector signal generator units, which shared a common reference clock [5]. The signals were upconverted to a centre frequency of 1575.42 MHz and amplified to a final transmit power of -16 dBm. The RF versions of *a(t)* and *b(t)*

were then, respectively, fed to the vertical antenna element of Sleds A and B. Accounting for free-space path loss, and the loss associate with linearly polarized broadcast antennas and circularly polarized receive antennas, the expected received power received at the array is approximately -75 dBm.

Data was collected using a quad-channel front-end, sampling at a rate of 2.5 MHz, complex, centred at 1575.42 MHz using the RHCP feed of antenna elements 1, 2, 4 and 6, as depicted in Figure 2. As the samples from the four channels were synchronous, the received samples from the four antenna elements were processed in a master-slave configuration, whereby the signals received at antenna element 1 were acquired and tracked using a modified software GNSS receiver, ant the samples from antenna elements 2 to 4 were simply demodulated using the same local signal replicas as that of antenna element 1. The receiver implemented a traditional parallel acquisition scheme and narrow-band delay- and phase-lock loops. Ultimately the receiver produced a set of 1 ms correlator dumps for each of the four antenna elements, for both signal *a(t)* and *b(t)*, wherein the correlator values corresponding to each of the slave antennas exhibit a scaling and rotation relative to the master antenna, resulting from the relative gain and phase response of each antenna, the difference in geometric distance, and the local oscillator phase at the front-end**.**

In this very controlled environment, the relative phase and amplitude of *a(t)* at each of the antenna elements can be very precisely determined and, so, accurately placing a null is relatively simple. In practice, however, when both the receiver transmitter are in motion, and the propagation channel may include multipath or fading, choosing appropriate values for κ and ϕ can be difficult. To explore the sensitivity the rejection level to the accuracy of these parameters, Sled A placed at -80° and Sled B at 0°, and a dataset of four minutes duration was recorded. The relative gain and phase between pairs of antenna elements was then precisely estimated. In this case, absolutely ideal propagation conditions, these parameters were effectively constant over the test duration.

Next, a null was placed in the direction of Sled A, but with intentional corruptions to the steering parameters κ and ϕ**.** The phase rotation was corrupted with a zero mean Gaussian random variable, to simulate errors in the estimate of the relative phase process, while a the gain parameter was multiplied by a Ricean random variable, to simulate errors in the estimation of the relative signal strength at each antenna, in terms of the signal-to-noise ratio of *a(t)*. Specifically, the null is placed according to:

$$\begin{aligned} & C_{i,j}(a, \kappa + \kappa_n, \pi + \phi + \phi_n) \\ & \phi_n \sim N\left(0, \sigma_\phi^2\right) \\ & \kappa_n \sim R\left(1, SNR^{-1}\right) \end{aligned} \tag{3}$$

where ***N*** and ***R*** respectively denote Gaussian and Rice distributions. The residual power of *a(t)* was then measured by computing the square magnitude of the average value of nulled correlator values over the entire four minute dataset. The measured signal rejection under these conditions are presented in Figure 3, assuming: a fixed signal SNR of 20 dB and a selection of phase standard deviation values ranging from 0.1 to 15° (left); and a fixed phase standard deviation of 1° and a selection of signal SNR values in the range 0 to 40 dB (right). It is clear that the rejection level is quite sensitive to errors in the estimate of phase, degrading by as much as 10 dB for errors as small as 1°. Similarly, the measured rejection level is quite sensitivity to amplitude, in particular when the signal to be rejected is observed at an SNR in the range of 0 to 20 dB. However, as these steering errors are reduced, the measured rejection level approaches 72 dB, corresponding to the maximum level that can be reliably measured in this case, given longer codes, or other means of providing higher separation between *a(t)* and *b(t)* it may be possible to observe higher rejections.

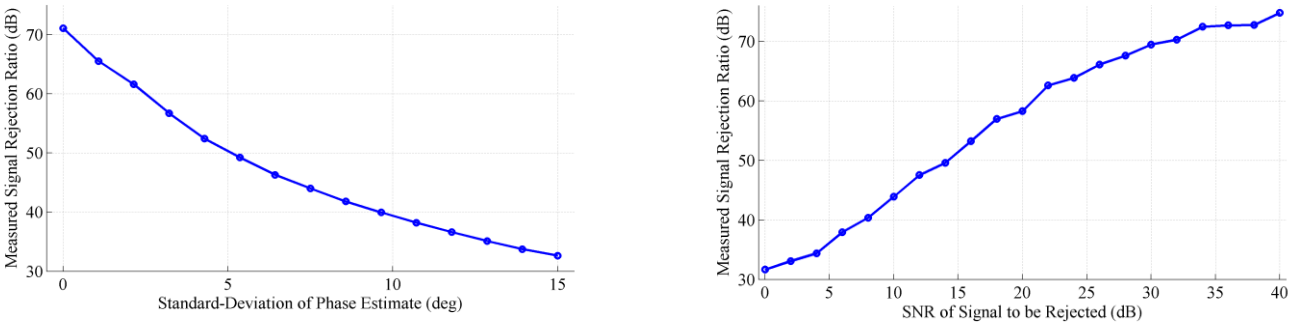

Figure 3: The measured rejection of an undesired signal power, relative to the desired signal power, as a function of the accuracy of the receivers estimate of the relative signal phase at two antennas (left), and as a function of the accuracy of the receivers estimate of the relative signal power at two antennas (right) .

REJECTION OF INTERFERENCE SIGNALS AT ANALGOUE RF

Having verified that the antenna array itself is capable, under very controlled conditions, of achieving very high rejection, this section proceeds to explore some of the receiver-side factors which can limit this performance. Here, the performance of an analogue RF combining circuit is examined, wherein the combining function, $C_{i,j}(s,\kappa,\phi)$ was implemented using controllable analogue attenuators and phase shifters. The received signal from each of two antennas, *i* and *j*, was fed to a custom RF circuit board hosting a controllable phase shifter and attenuator chips [6,7]. The output of two of these boards was then combined using a passive power combiner, filtered by an analogue RF filter, limiting the band to the range 1530.0 to 1620.0 MHz, and finally fed to a power detector which produced a signal voltage which was proportional to the total observed power. The experimental setup is depicted in Figure 4 (left). The attenuators and phase shifters were controlled digitally via an Arduino interface and controller board [8], which also sampled the output of the power detector. The attenuators accept a 6-bit control, providing a dynamic range of 30 dB in steps of approximately 0.5 dB, while the phase shifters accept a 4-bit control traversing the unit circle in steps of 22.5°.

Unlike the previous case, where significant care had to be taken not to saturate the amplification stages or to drive the digitizers out of their nominal operating region, these components exhibit a very high linear region and can tolerate strong interference signals. For this reason, the power of the unwanted signal, *a(t)*, could be measured directly, both before and after placing the null and a simple continuous wave signal could be used. To investigate the performance of the system, a continuous wave interference was broadcast toward the array, while signal from one antenna was manipulated by all possible gain and phase combinations, keeping the signal from the second antenna at a fixed zero phase shift and -15 dB attenuation. For each of the 1024 possible gain and phase combinations, the power detector was sampled and logged. A trace of the measured signal rejection as a function of the gain and phase is depicted in Figure 4 (right), wherein a sharp peak is observable at approximately {-15 dB, 210°}, corresponding to the point at which the unwanted signal is rejected was most rejection, in this particular to a level of approximately 29 dB.

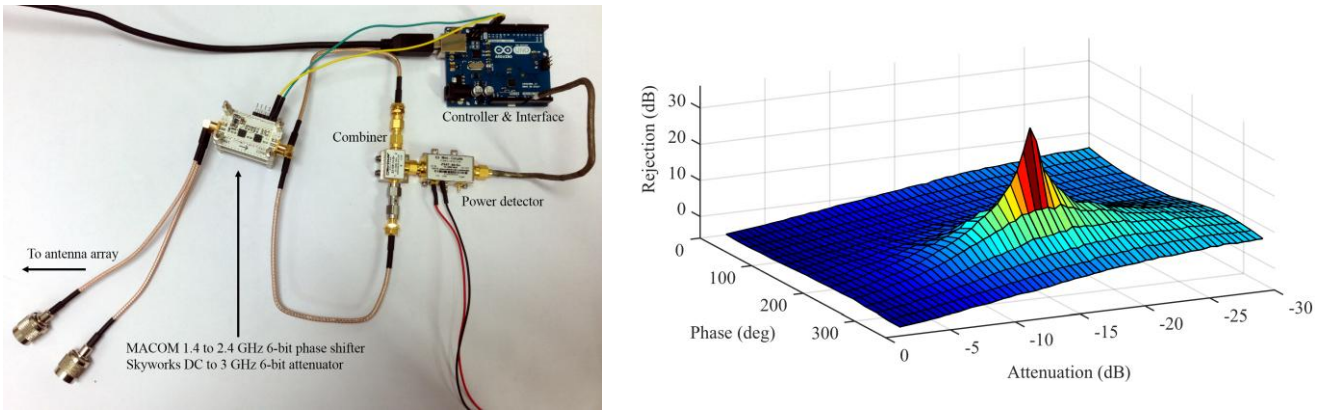

Figure 4 A custom built programmable analogue phase shifter and attenuator pair used for the analogue null-steering configuration (left), and the measured interference rejection level as a function of phase and attenuation, for a broadcast jamming scenario (right).

In this particular experiment, because all 1024 possible gain and phase combinations were examined in a brute-force search, the signal rejection was not limited by inaccuracies in the estimation of the steering variables κ and ϕ, rather, it is a limited by how accurately they can be applied. A residual error exists between the phase and gain that would perfectly align and null the signal, and the nearest values that can be applied by the circuit. This error is a function of the distribution of the true steering parameter and the resolution with which it is rendered. In this case, as the range and angle to the unwanted signal source is arbitrary and the distance between antenna elements is comparable to the carrier wavelength, then it is, perhaps, reasonable to assume that the residual error in the steering parameters is zero mean, and uniform over the discrete control steps. To model this effect, similar to the previous section, the combining function, inclusive of these errors can be expressed as:

$$\begin{aligned} & C_{i,j}(a,\kappa+\kappa_u,\pi+\phi+\phi_u) \\ & \phi_u \sim U\left(-\delta\phi/2,\delta\phi/2\right) \\ & \kappa_u \sim U\left(\delta A^{-1/4},\delta A^{1/4}\right), \end{aligned} \tag{4}$$

where *U* denotes a uniform distribution, and *B* denotes the number of bits used in the phase shifter control and δA denotes the attenuator step size. Note that as κ is in units of amplitude and δA represents the discrete steps in power

gain, which corresponds to discrete steps of $\sqrt{\delta A}$ in amplitude, then the residual error will be distributed over a region extending $\sqrt[4]{\delta A}$ in either direction. In this case if a B-bit phase shifter is sued, then:

$$\delta\phi = \frac{2\pi}{2^B}. \tag{5}$$

From this model, the minimum expected rejection level can be estimated, as a function of the phase and attenuator resolution. Examining **(4)** and **(2)**, it is clear that the minimum rejection will be achieved when the residual phase error is equal to $\delta\phi/2$ and amplitude mismatch is equal to $\sqrt{\delta A}$. Thus, the minimum, and average expected rejection is given by:

$$\min_{\phi_u,\kappa_u}\{R_{a,b}\} = \frac{1}{1+\sqrt{\delta A}-2\sqrt[4]{\delta A}\cos\left(\delta\phi/2\right)}. \tag{6}$$

$$\left\langle R_{a,b}\right\rangle_{\phi_u,\kappa_u} = \frac{3\left(1+\sqrt{\delta A}\right)^3\delta\phi - 16\sqrt[4]{\delta A}\left(1+\sqrt{\delta A}+\delta A\right)\sin\left(\delta\phi/2\right)}{6\left(\delta A+\sqrt{\delta A}\right)\delta\phi}. \tag{7}$$

Inserting the specifications of the experimental setup used here, we find that the minimum rejection that can be expected rejection level is equal to approximately 14 dB with an average value equal to 18.8 dB. Further exploring this result, it is possible to predict the minimum performance that can be achieved given some arbitrary, but finite, resolution in gain and phase rotation. A portion of the surface defined by **(7)** is presented in Figure 5. One useful application of this result in ensuring that the resolution in gain and in phase are commensurate. This can be inferred by examining the gradient of the surface, noting that optimal choices of gain and phase step size will lie along the line of steepest gradient of this surface. A flattening of the surface in one dimension indicates that the performance is limited by the other dimension. For example, it can be seen that an increase in phase resolution beyond 6-bits yields no improvement in rejection when the gain step size is greater than 0.5 dB.

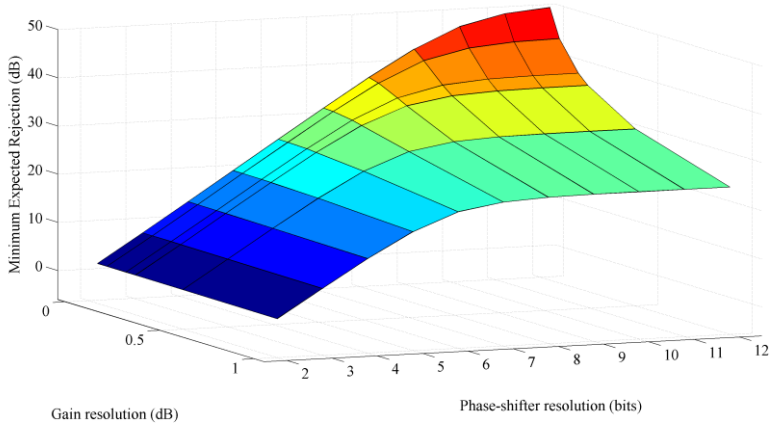

Figure 5: Minimum achievable rejection of analogue nulling-combiner as a function of phase-shifter resolution (bits) and attenuator step size (dB)

DIGITIZATION EFFECTS: REJECTION OF INTERFERENCE SIGNALS AT DIGITAL IF

Unlike the analog combination of signals at RF, which typically can tolerate very high interference power levels while maintaining linear operation, when the combining operation, **(1)**, is implemented post digitization, the resolution with which digital samples are represented has a significant impact on the achievable rejection. Moreover, due to saturation of the digitizers, and their limited capacity to represent signals with a very large dynamic range, a direct measure of the rejection achieved by placing a null is difficult to measure. To avoid this challenge, the rejection performance can be assessed in terms of an indirect signal quality metric, the bit error rate (BER) [9,10]. In this section, the BER observed

on a single GPS L1 C/A signal is measured in the presence of continuous wave interference signal emanating from a source separated by 60° in azimuth from the satellite.

Via Monte-Carlo simulation, the BER was estimated over a 600 second trial for a single-antenna configuration, and for a dual-antenna configuration which placed a null in the direction of the interference. The sample rate was set to 4 MHz complex, the GPS signal was assumed to be received at a C/N_0 of 50 dBHz, and a continuous wave interference was placed at random frequency, for each bit of the L1 C/A signal, on an interval spanning 40 kHz around the GPS center frequency. The standard-deviation of the receivers estimate of the received phase-difference between antennas was assumed to be 1°, and the estimate of the relative power was assumed have an SNR of 26 dB (see Figure 3). The trial was repeated for a range of interference-to-noise power scenarios and for 1-, 2-, 3- and 4-bit receivers and the non-digitizing receiver, representing an ideal upper bound. In each case, a classical gain-control algorithm was implemented which produced a simple measure of the IF power, and tuned the digitizer thresholds under the blind assumption that the power was Gaussian in distribution 11]. A selection of the results are presented in Figure 6.

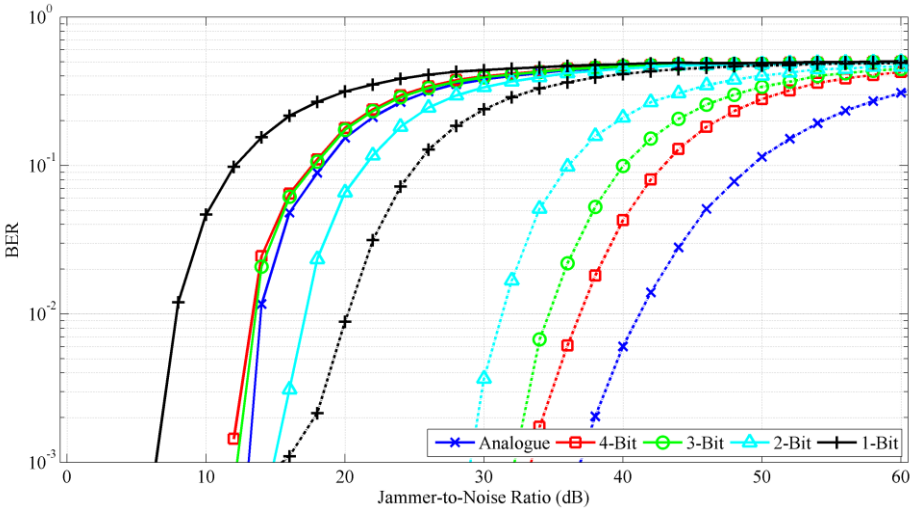

Figure 6: Bit-error-rate versus interference strength for the single-antenna configuration (solid lines) and the nulling case (broken lines) for digitizers ranging from one- to four-bit resolution and the ideal, analogue case.

To glean some insight into the sensitivity of the nulling performance to the number of bits used in the digitizer it is interesting to examine the relative interference powers that inflict a given BER for the single-antenna configuration, to that of the dual-antenna nulling case. For example, examining the 1-bit curves, a BER of 10^{-2} is measured for a JNR of approximately 8 dB for the single-antenna configuration, and at approximately 20 dB once a null is placed, suggesting that when a 1-bit digitizer is used, the rejection level is limited to an effective value of 12.4 dB. When a 2-bit digitizer is employed this effective rejection increases to approximately 13.5 dB, and further increases to 21.1 and 23.35 dB, respectively, for 3- and 4-bit digitizers, ultimately saturating at 27.62 dB in the non-digitizing case. Of course, care must be taken not to interpret these figures directly as effective reductions in the interference power, as presented in Figure 3, as these particular results represent an average BER for a wide range of interference frequencies, with some particular interference frequencies inducing the most bit errors.

Nonetheless, these results may offer some insight into digitizer choice. In the single-antenna case, it appears as though little improvement is gained by increasing the digitizer resolution beyond a 3-bit digitizer in the presence of strong interference, confirming a result previously shown in [10]. In contrast, when placing a null in the direction of the interference, the achievable rejection appears to increase steadily with increased digitizer resolution from 3- to 4-bit and onwards to the non-digitizing case. This suggests that the mechanism which limits the BER improvement with increased resolution in the single antenna case does not apply in the exact same manner in the multi-antenna case. Determining exactly what digitizer resolution should be used, or where the benefits of increased resolution plateaus, is beyond the scope of this study. Moreover, BER is only one of many parameters by which this improvement might be measured, however, and further metrics such as detection probability, receiver operating characteristic, tracking threshold might be investigated [9,10,11].

CONCLUSIONS

Early results from this study suggest that the achievable signal rejection using a controlled radiation pattern GNSS antenna, under ideal conditions, is in excess of 70 dB, and is primarily limited by the accuracy with which the angle of incidence of the interference can be estimated. Accounting for typical estimation errors, the nominal rejection levels of the order of 20 to 40 dB can be expected. Other aspects which limit the signal rejection performance, in a practical receiver, stem from component selection for the signal combining circuitry. One factor is the resolution of the controlled attenuators and phase shifters used in analogue combining schemes, the minimum expected performance of which has been characterized by a theoretical model presented herein. Further work will focus on extending the current results to consider the multi-null case and the use of Another factor, relating to post-digitizer combining schemes, is the resolution of the digitizers employed. It is apparent that the achievable rejection level is severely hampered by the use of low-resolution digitizers, being limited to 12 dB in the case of a 1-bit digitizer, but increases dramatically when three or more bits are used. Further work is required to more precisely determine the role of the digitizer in multi-antenna signal rejection schemes: to identify the appropriate gain control, and to further understand and quantify the effective loss in signal rejection capability.

REFERENCES

[1] Antcom, "RHCP/LHCP L1/L2GPS Antenna, P/N: 3G1215RL-PP-XS-X," *http://www.antcom.com* RHCP-LHCP-V-H-L1L2GPSAntennas.pdf, [Accessed March 2015]

[2] Tallysman Wireless, "TW127 1559 MHz to 1610 MHz 25dB In-line Amplifier," *http://www.tallysman.com/TW127.php*, [Accessed March 2015]

[3] Agilent , "Agilent Network E8361A PNA Network Analyzer, 10 MHz to 50 GHz", http://www.keysight.com/, [Accessed March 2015]

[4] E. Kaplan, Ed., "Understandin GPS, Principles and Applications," Artech House Publishers, 1996.

[5] National Instruments, "NI PXIe-5672 2.7 GHz Vector Signal Generator," http://sine.ni.com/nips/cds/view/p/lang/it/nid/203928, [Accessed March 2015]

[6] MACOM, "MAPS-010143", http://cdn.macom.com/datasheets/MAPS-010143_V2.pdf, [Accessed March 2015]

[7] Skyworks, "SKY12347-362LF: DC-3.0 GHz Six-Bit Digital Attenuator," http://www.skyworksinc.com/uploads/documents/201371B.pdf, [Accessed March 2015]

[8] Arduino, "Arduino Uno Microcontroller," http://arduino.cc/en/main/arduinoBoardUno, [Accessed March 2015]

[9] J. Arribas et al, "Antenna Array Based GNSS Signal Acquisition for Interference Mitigation," Aerospace and Electronic Systems, IEEE Transactions on, vol. 49, no. 1, Jan 2013

[10] M. Abdizadeh et al, "New Decision Variables for GNSS Acquisition in the Presence of CW Interference," Aerospace and Electronic Systems, IEEE Transactions on, In Press, 2014

[11] M. Abdizadeh et al, "Quantization Effects in GNSS Receivers in The Presence of Interference", ION International Technical Meeting 2012, Newport Beach, CA, Jan 30 – Feb 1